Extended X-Ray Reflectivity Analysis of Si(111)7×7

I.K. Robinson and E. Vlieg

AT&T Bell Laboratories, Murray Hill, NJ 07974, USA

A number of new results are emerging from the various techniques for measurement of surfaces using X-ray and neutron scattering methods, as witnessed by the program of this conference. With many names (and thankfully few acronyms) currently in use for these methods, it can be helpful to summarise them according to the regions of reciprocal space they refer to, as we attempt to do in Fig 1. This forms a useful guide to evaluating the level of information attained in each experiment, with regard to resolution of detail and its direction. The principal distinction is between the reflectivity ($Q_\parallel \approx 0$) and diffraction ($Q_\parallel >> 0$) regions; further subdivisions apply when $Q_\perp \approx 0$ or not, as shown. A finer distinction could have been made between the analysis of crystal truncation rods ("integer order" diffraction) and superstructure reflections (fractional orders), but we chose not to show this.

In this paper we concentrate on the interpretation of reflectivity data. The conventional view of X-ray reflectivity is understood to be represented by the Fresnel law, and the deviations from it which may have structural interpretations [1]. The *non-specular* reflectivity region is the surface equivalent of small angle scattering. Here the collective modes of fluid surfaces, in the form of capillary waves, are detected [2]. In the reflectivity region far from the origin where the crystalline Bragg peaks start to appear, the simple dielectric boundary description of the Fresnel law no longer applies. In order to separate its identity we refer to this as the *extended reflectivity* region.

In the extended reflectivity region the refraction effects near $Q_\perp = 0$ are unimportant, and the kinematic approach analogous to the analysis of crystal

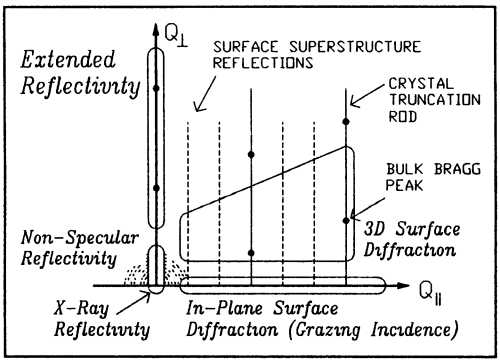

Figure 1. Schematic map of surface scattering methods in reciprocal space.

Springer Proceedings in Physics, Vol. 61 **Surface X-Ray and Neutron Scattering**
Eds.: H. Zabel and I.K. Robinson

truncation rods (CTRs) [3] is appropriate, except that all lateral order within the layers of the sample is invisible. The scattering amplitude can be represented as a one-dimensional sum over the layers of the crystal from the top (z = 0) to z = ∞. Quite generally we can represent each layer by an index j, a position z_j, and a density ρ_j (fractional occupancy between 0 and 1):

$$F(Q) = f(Q) \sum_{j=0}^{\infty} \rho_j e^{iQz_j} \qquad (1)$$

where f(Q) is the known form factor, and can be used to include overall scale and Debye-Waller factors as well. An ideal primitive lattice is represented by $\rho_j = 1$ and $z_j = ja$, where a is the perpendicular lattice parameter. Equ 1 reduces to

$$|F(Q)|^2 = \frac{|f(Q)|^2}{\sin^2 \tfrac{1}{2} Qa} \qquad (2)$$

demonstrating the $1/\sin^2$ intensity variation characteristic of CTRs. Close to the Bragg peaks at $Q = 2\pi n/a$, the intensity has the asymptotic form $1/|\Delta Q|^2$ that was originally derived by von Laue for the effect of plate morphology on powder diffraction [4], and later for surfaces [5]. It is curious to note that the intensity variation of Equ 2 can be obtained exactly by summing the $1/|\Delta Q|^2$ singularities over all the Bragg peaks, by virtue of the equality

$$\frac{1}{\sin^2 \pi x} = \frac{1}{\pi^2} \sum_{n=-\infty}^{\infty} \frac{1}{(x-n)^2} \; . \qquad (3)$$

This has led to an alternative description [6] of extended reflectivity, and CTRs in general, as a superposition of $1/|\Delta Q|^2$ *intensity* tails weighted by the squares of the structure factor at each Bragg peak.

We wish to point out that this equivalence of the two derivations breaks down when the crystal structure is sufficiently complicated. The generalisation of equation (3) works for the case of a primitive lattice of layers with equal weight, AAAA... It also works for an ABABAB... structure, but not for one with a non-uniform layer spacing, such as Si(111), which is illustrated in fig 2. There exist two possible 'ideal' terminations: case 'D' cutting between the double-layers of atoms, and case 'S' splitting the double layer. Fig 2 also shows the extended reflectivity calculated by the two methods. All curves reproduce the correct intensity ratio 2:1:0:1:2 for the (000):(111):(222):(333):(444) Bragg peaks of the diamond lattice. Away from the Bragg peaks they differ, however: in case 'S' there are nodes of zero intensity along the rod profile, but not in 'D'. The superposition of tails calculation generates a curve lying in between, *which is independent of choice of termination.* The differences are not slight: there is almost a factor of 10 difference over most of the region near (222). Very clearly, the profile is sensitive to the choice of termination.

The real Si(111) surface is reconstructed in a way that is described by the well-known 7x7 Dimer-Adatom-Stacking fault (DAS) model [7], shown in a side view in fig 3. This is a relatively complex structure with a reflectivity profile that

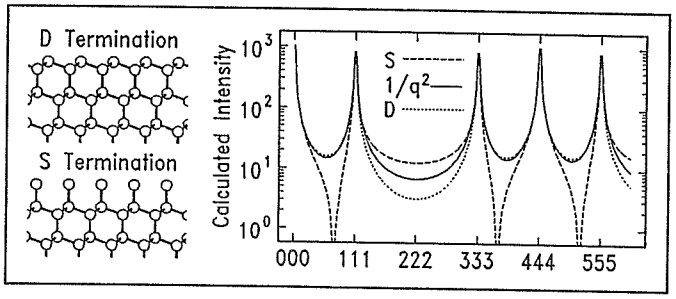

Figure 2. Left: notation for the two possible 'ideal' terminations of the Si lattice by a (111) plane. Right: calculated truncation rod intensity profiles for these ('S' and 'D') with the curve obtained using the sum of intensity tails [6].

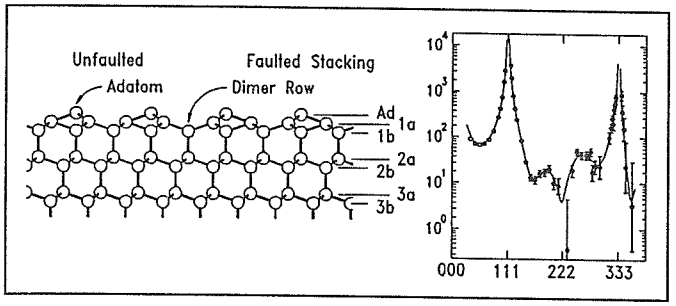

Figure 3. Left: side view of the Dimer Adatom Stacking-fault (DAS) model of the reconstructed Si(111)7x7 surface. Right: measured extended x-ray reflectivity as a function of $Q_\perp$ (bulk Miller index units) and the best fit curve.

would be neither 'S' nor 'D'. Although the general model is no longer questioned, the determination of the structure at the level of atomic positions is still making progress, with recent contributions from Low Energy Electron Diffraction [8] (LEED), Reflection High Energy Electron Diffraction [9] (RHEED) and in-plane x-ray diffraction [10]. As more accurate positions become available, more of the subtle roles of strain and variations in local coordination can be explored [11]. Until now there is no accurate total energy calculation and coordinate optimization of the 7x7 structure because the size of such a project is too large for present day computers, and even this would not answer all the structural questions: the penetration of the strain fields far inside the bulk, for example. The best theoretical prediction of the structure so far comes from a local density approximation (LDA) theory in a 2x2 unit cell [12].

We measured the extended reflectivity of Si(111)7x7 on beamline X16A of the National Synchrotron Light Source (NSLS) at Brookhaven National Laboratory using a UHV x-ray diffractometer [13]. The measurements were made with the detector resolution defined by 2x2mm slits 500mm from the sample and a beam of 2mm in height. At small angle the slits were reduced to 1x1mm and 1mm respectively to avoid running off the sample, and the data were

rescaled. The sample was mounted with the diffractometer axis lying in the surface plane, *i.e.* 90° away from the usual setting [13]. In this way a large range of momentum transfers was obtained. The sample was prepared by chemical oxidation using the Shiraki [14] method, followed by resistive heating to about 1200° C to yield a 7x7 LEED pattern.

Data were collected for each point on the reflectivity profile as scans of the diffractometer ω-axis sufficiently far to reach background. The peak was numerically integrated and background subtracted. No trend in the shapes of the peaks was observed; they were always resolution-limited. Data were also taken by scanning in the perpendicular χ direction [13] yielding consistent results. Each intensity point was multiplied by $\sin 2\Theta$, which is the appropriate Lorentz factor; no polarization correction was needed because of the vertical scattering geometry. A second multiplication by $\sin 2\Theta$ represents the variation of sample area with diffraction angle. Error bars for each point were estimated as a quadrature combination of counting statistics plus a 5% systematic error, found to represent repeated measurements with different alignment, scan direction and slit settings. The full set of measured intensities is shown as the points on figure 3. The 111 and 333 Bragg peaks of Si are clearly seen as divergences of the intensity; no attempt was made to measure closer to these, since resolution and detector saturation effects would start to become important.

The theoretical curve that fits the data in fig 3 is eq(1), modified to include a layerwise Debye-Waller-like 'thickness' term, $\exp(-\frac{1}{2}q^2\zeta_j^2)$, representing the variation of heights within each layer of the structure. The layer occupancies, ρ_j, were taken directly from the DAS model, while the heights, z_j, were adjusted for layers 'Ad' to '3b' in fig 3. The final parameters gave a χ^2 of 0.94. The parameter values and their relation to those obtained by other methods [8,9,12] are discussed elsewhere [15]. There are several oscillations in the curve that arise from the presence of the adatoms (fig 3) and from an expansion of the top layer spacing. The expansion was seen in the LDA calculation [12], but not in LEED [8] or RHEED [9], perhaps because of the limited depth penetration of these electron-based techniques.

NSLS is supported by the U.S. Department of Energy under grant DE-AC012-76CH00016.

References

1. J. Als-Nielsen, in *Handbook on Synchrotron Radiation*, vol. III, ed. D. E. Moncton and G. S. Brown (Elsevier, North-Holland, 1991).
2. M. K. Sanyal, S. K. Sinha, K. G. Huang and B. M. Ocko, Phys. Rev. Lett. **66** 628 (1991); S. K. Sinha, these proceedings (following paper).
3. I. K. Robinson, Phys. Rev. B **33** 3830 (1986).
4. M. von Laue, Annalen d. Physik (folge V) **26** 62 (1936).
5. S. R. Andrews and R. A. Cowley, J. Phys. C **18** 6427 (1985).
6. H. You, these proceedings and private communication.

7. K. Takayanagi, Y. Tanishiro, S. Takahashi and M. Takahashi, Surface Sci. **164** 367 (1985).
8. H. Huang, S. Y. Tong, W. E. Packard and M. B. Webb, Phys. Lett. A **130** 166 (1988).
9. A. Ichimiya, Surf. Sci. **192** L893 (1987).
10. I. K. Robinson, W. K. Waskiewicz, P. H. Fuoss and L. J. Norton, Phys. Rev. B **37** 4325 (1988).
11. M. C. Payne, J. Phys. C **20** L983 (1987); I. K. Robinson, J. Vacuum Science Technology A**6** 1966 (1988).
12. R. D. Meade and D. Vanderbilt, Phys. Rev. B **40** 3905 (1989).
13. P. H. Fuoss and I. K. Robinson, Nucl. Inst. Meth. **222** 171 (1984).
14. A. Ishizaka, N. Nakagawa and Y. Shiraki, in *Proc. 2nd Int. Symp. on MBE and Related Clean Surface Techniques*, 183 (JSAP, Tokyo, 1982).
15. I. K. Robinson and E. Vlieg, submitted to Phys. Rev. B.